



Formation of pre-coating dynamic membrane on mesh filter by cross-flow filtration of PAC–water suspension in a bioreactor: experimental and modeling

Amir Ali Poostchi, Mitra Bayat, Maryam Rezaei, Ershad Amini,
Mohammad Reza Mehrnia*

School of Chemical Engineering, College of Engineering, University of Tehran, P.O. Box 11155-4563, Tehran, Iran, Tel. +98 21 61112184; Fax: +98 21 6695404; email: mmehrnian@ut.ac.ir

Received 13 November 2013; Accepted 29 March 2014

ABSTRACT

This study presents a closed-loop process for forming pre-coated dynamic membrane used in membrane bioreactor. Powder-activated carbon (PAC) particles are suspended by using axial-flow agitator whilst simultaneously deposited upon the filter medium by cross-flow filtration. The revolution speed of agitator is varied in the range of 150–450 rpm. Computational fluid dynamic is used to calculate velocity and shear rate adjacent to membrane surface. The force balance of the particles considers the driving force of dynamic membrane formation, drag force due to negative pressure-driven of suction pump, lift force due to mechanical mixing, and adhesive force due to particle–particle interactions. The effect of two major terms including drag and lift forces on the porosity of dynamic membrane is systematically investigated. The lower drag force results in the higher porosity of dynamic membrane. The results also show that the denser dynamic membrane is formed when the lift force becomes lower. The porosity of dynamic membrane is ranged from 0.38 to 0.46 while the thickness of dynamic membrane is altered between 100 and 500 μm . A dimensionless immobilized parameter is derived to predict the formation of pre-coating dynamic membrane. The results obtained from modeling show that dynamic membranes formed at higher values of immobilization parameter have a more cohesive structure. The results obtained from the experiments and the model reveal that the thickness of 400 μm of PAC layer is considered as a stability threshold thereafter the structure of dynamic membrane becomes loose and unstable. The rejection capacity of dynamic membrane is also evaluated at different thicknesses by using Formazin solution. The results reveal that the turbidity of filtrate decreases with increasing the thickness of dynamic membrane. The results display that rejection capacity of pre-coating dynamic membrane is comparable to that of microfiltration membrane.

Key words: Pre-coating process; Membrane bioreactor; Powder-activated carbon; Mesh filter

1. Introduction

Membrane bioreactor (MBR), integrating separation process and biological degradation, has widely been

used as a proven technology in treating both domestic and industrial wastewater [1,2]. The formation of cake layer so-called fouling upon the surface of conventional polymeric membranes makes a substantial drawback for industrially widespread application of

*Corresponding author.

MBRs [3,4]. Dynamic membrane technology represents a promising substitution for conventional membrane bioreactor, which owns the merits of flexible and cheap materials, easy for cleaning, and good antifouling property [5,6]. Chu et al. [7] showed that dynamic membrane bioreactor exhibited excellent operation performance and could be considered as a feasible and potential approach to wastewater treatment. The concept of the dynamic membrane formation is based on the continuous deposition of the suspended particles upon the external surface and or onto the porous media as well as membrane and filter medium. Two well-known methods, pre-coating and self-forming, are ordinarily established in order to create the dynamic membrane in MBRs [8]. The pre-coating dynamic membrane is being created when a porous medium is submerged in a bioreactor and the solid particles dispersed into the liquid phase gradually deposit upon the porous surface. The self-forming dynamic membrane is created by substances such as colloids and high molecular weight organics which exist in the liquor to be filtered. Most of studies related to dynamic membrane bioreactor have been established in the mechanism and performance of self-forming dynamic membrane for wastewater treatment [9–14]. But there has been limited information about mechanism and process of pre-coating dynamic membrane. Chu et al. [15] investigated the pre-coating process for formation of bio-diatomite dynamic membrane bioreactor under a constant water head. They also evaluated the pollutant removal mechanisms in a bio-diatomite reactor to purify the micropolluted surface water [16]. In earlier studies especial attention has been received to the thickness of pre-coating dynamic membrane [8,17]. Chu et al. [18] investigated the characteristics of bio-enhanced powder-activated carbon (PAC) dynamic membrane reactor for municipal wastewater treatment. They showed that the dynamic membrane formed on the stainless steel mesh filter could effectively reject the suspended solids. However, the porosity of dynamic membrane can mostly influence the performance of dynamic membrane bioreactor. The architectural feature of the pre-coating dynamic membrane such as porosity is in close association with its specific resistance and thus, directly related to the membrane permeability in an MBR. In the present study, a reliable *in situ* pre-coating technique is presented by using both mesh filter medium submerged in bioreactor and PAC mechanically suspended throughout bioreactor. In particular, addition of PAC to MBR brings about some positive effects including prevention of particle deposition on the membrane surface [19], formation of a less compressible cake or gel layer [20], adsorption of

membrane foulants such as soluble extracellular polymeric substances [21,22], promotion of the performance of MBRs in terms of the quality of treated water [23], and pretreatment of micropolluted surface water to produce drinking water [24]. The model is also proposed to predict condition of PAC particle deposition based on the forces associated to a suspended particle that is sufficiently close to a stationary particle in the dynamic membrane layer. Three forces including lift force due to mechanical mixing; drag force due to pump suction; and adhesive force due to particle–particle interactions are taken into account in prediction of deposition of PAC particles in the accumulated particle layer. Since computational fluid dynamics (CFD) is a powerful tool to estimate the characteristics which cannot be measured experimentally, so in this study CFD simulation is implemented to determine the velocity and the shear rate distribution near the dynamic membrane surface. The validation of the model is performed according to the experimental data obtained during formation of pre-coating dynamic membrane.

2. Materials and methods

2.1. Experimental setup

The schematic diagram of experimental setup and the pre-coating dynamic membrane formed are illustrated in Fig. 1. Bioreactor is a rectangular Plexiglas vessel and has a 0.17 m width, 0.2 m length, and 0.5 m height. The suspension of PAC particles throughout the volume of bioreactor is ensured by a down-flow axial agitator driven by a DC electromotor with a digitally monitored speed controller. Monofilament mesh filter made of polyester is used with average pore size of 30 μm . A rectangular holding frame made of polyethylene is constructed to tightly support filter for no-leakage. The filter medium with its holding frame is vertically placed in the center of bioreactor. The pressure drop across the filter medium is measured by a high accurate sensor installed in the filtrate line as close as possible to the filter module. The sensor is connected to the on-board controller and analog to digital card (I/O module) in order to transmit the digital signals to a PC for data gathering and acquisition. Data are collected and recorded on dedicated log sheets during the experiments. A peristaltic pump which operates at constant flux of 150 ($\text{L}/\text{m}^2\text{h}$) is used to suck and recycle the water back to the bioreactor. The rate of filtrate is timely monitored by the use of a calibrated flow meter. PAC particles with average mean diameter 100 μm are used to form the pre-coating dynamic membrane. The concentrations of PAC

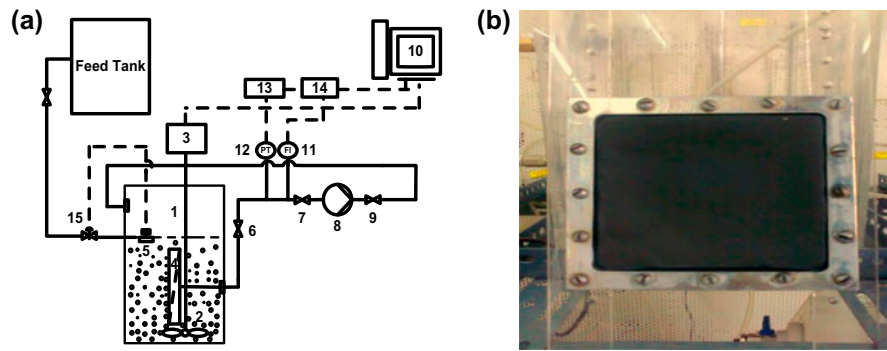


Fig. 1. (a) process flow diagram: (1) Bioreactor vessel; (2) Axial agitator; (3) DC electrical motor; (4) Filter module; (5) Level switch; (6) Permeate valve; (7) Inlet pump valve; (8) Permeate pump; (9) Outlet pump valve; (10). Computer system; (11) Flow indicator; (12) Pressure transmitter; (13) I/O module; (14) Flow transmitter; (15) Control valve, (b) dynamic membrane formed by PAC deposition on mesh filter medium.

particles suspended into the volume of bioreactor are between 0.25 and 1.1 g/L. The rate of PAC dosage is sufficient to form the pre-coating dynamic membrane at different thicknesses. Prior to use PAC particles in experiments, they are rinsed by using distilled water to remove any fines and dried in the oven at 105°C. The detail characteristics of commercial PAC particles are presented in Table 1. In order to compare the capacity of dynamic membrane in rejecting matter with conventional membrane used in MBR systems, a flat sheet microfiltration membrane made of polyvinylidene fluoride (PVDF) is used with mean pore size 0.20 µm.

2.2. Field emission scanning electron microscopy

The surface of dynamic membrane layer formed on the mesh filter with corresponding cross-section structure is observed with the help of a scanning electron microscopy (S4160, Hitachi, Japan). The boundary between the filter and the dynamic membrane is readily distinguishable, so the thickness of the PAC layer is easily determined. When forming the dynamic membrane, the suction pump is stopped and the permeate valve is normally closed to prevent the back

flow of the filtrate due to built-up back pressure. The sample of pre-coating dynamic membrane is precisely obtained and accurately fixed to the welfare of the SEM. When separating the piece of PAC particle layer from the mesh filter, especial attention must be given to preserving the origin of the microstructure. A coating of gold by a sputter is set on the sample in order to increase surface resolution.

2.3. Porosity measurement

The porosity of dynamic membrane formed is determined by using two methods, direct and optical. In direct method, the mass of bare mesh filter is determined prior to PAC deposition. The mass of PAC layer is calculated by subtracting two obtained masses, the mass of PAC layer with mesh filter and the mass of bare mesh filter. The volume of the PAC layer is determined by dividing the mass to bulk density of PAC. Total volume of dynamic membrane is determined by measurement of the height of PAC layer using SEM. Porosity is measured by dividing pore volume obtained to total volume of dynamic membrane. In the optical method, the SEM images taken from the cross-sectional view of dynamic membrane is analyzed using Image J 1.46 software. This software utilizes the contrast between two phases, pores and PAC part, in the SEM Image. Fig. 2(b) shows the scanned image of the cross-sectional view of dynamic membrane obtained from SEM observation, Fig. 2(a). As shown in Fig. 2(b), pore areas are extracted using Image J software (blue lines). The porosity based on area fraction for the dynamic membrane is then determined. The porosity value obtained from direct and optical methods becomes 0.405 and 0.401, respectively, for dynamic membrane with thickness 300 µm.

Table 1
The characteristics of PAC

Specification	Unit	Quantity
Mean particle size	mm	0.1
Iodine number	mg/g	950
Surface area, BET (N ₂ /77°K)	m ² /gr	1,055
pH	–	6–8
Ash content	%wt	2–3

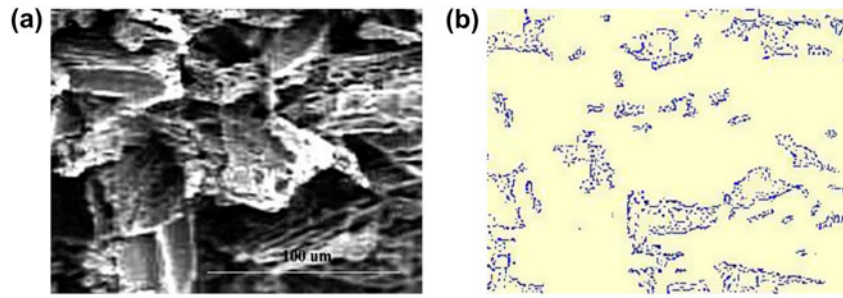


Fig. 2. (a) SEM image of dynamic membrane, (b) pore areas extracted by using Image J software.

2.4. CFD simulation

Since the bioreactor is equipped with the mesh filter and the agitator, so the multiple reference frame (MRF) model as well as Navier-Stokes method with $k-\varepsilon$ turbulence model is applied. The MRF method simulates the flow for fixed position of the agitator relative to the vessel [25,26]. In this method the solution domain is divided into two regions, namely, inner and outer region. For the inner region the continuity and the momentum equations are solved in rotating framework as well as agitator and for the outer region those equations are solved in the stationary framework as well as mesh filter [27]. The assumptions required for CFD simulation using Fluent 6.3.26 software and the numerical implementation has been explained in detail at the study which has been previously done [28].

3. Theoretical modeling

The conditions under which pre-coating dynamic membrane is formed are based on some assumptions to be expressed as following:

- (1) The dynamic membrane is growing in the z -direction as shown in Fig. 3.
- (2) The particle size of PAC is equal to $100\ \mu\text{m}$ and the shape of PAC is imagined as spherical particle with smooth external surface.
- (3) The spherical particles suspended through the volume of the bioreactor are assumed to be mono-dispersed.
- (4) The fluid flow around each stationary particle in the PAC deposit layer is assumed to be identical.
- (5) The effect of filter surface on the adhesive forces including Van der Waals and electrostatic forces is assumed to be negligible.
- (6) The mechanisms of the filtration are assumed to be the surface straining and the cake filtration.
- (7) The dynamic membrane is considered as an

incompressible layer and a cubic structure as shown in SEM images, Fig. 4.

The three forces including lift due to mechanical mixing, drag due to negative pressure-driven filtration, and adhesive due to particle–particle interactions are taken into account in prediction of PAC particle deposition upon the mesh filter. The adhesive force plays a significant role in attaching the particles to dynamic membrane layer, specifically for fine particles with diameter less than $100\ \mu\text{m}$ [29]. Fig. 3 shows the forces acting on the particle B that becomes very close to the stationary particle A . The particles settled in the dynamic membrane layer are also under a stress created by the filtrate flow. The drag force acted on a particle existing in the dynamic membrane can be approximated by following equation [30]:

$$F_D = kd^2\mu\frac{u}{d} \quad (1)$$

when k value is equal to 3π , it becomes valid for a viscous fluid flow around a single particle. Neesse et al. [29] estimated the quantity of k approached to unit for filter media. The total drag force acting on particle A at a specific layer of the dynamic membrane, ($\delta = L-Z$), is assumed as below:

$$F_d^{(A)} = kd\mu u \left(\frac{\delta}{d} \right) \quad (2)$$

δ is assumed to be equal to two mono-layers of PAC particle at the external surface of dynamic membrane. In addition to drag force, the pressure drop across the dynamic membrane can be expressed by following equation [31]:

$$\Delta P \approx (1 - \varepsilon)f(\varepsilon)\frac{L}{d^2}\mu u \quad (3)$$

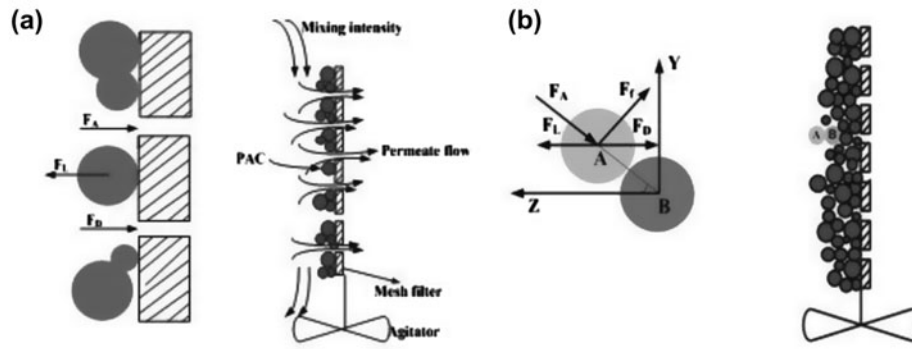


Fig. 3. (a) deposition of PAC on the surface of mesh and the flow patterns, (b) deposition of PAC on the dynamic membrane and the forces acting on a PAC particle depositing.

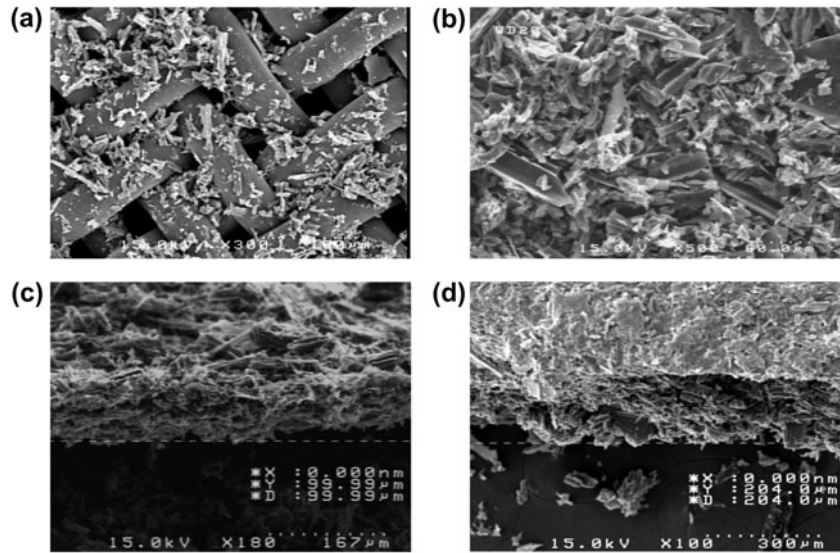


Fig. 4. (a) deposition of PAC particles onto the yarns of mesh filter, (b) surface of the dynamic membrane formed, (c) dynamic membrane formed at thickness of 100 μm, and (d) dynamic membrane formed at thickness of 200 μm.

where $f(\varepsilon)$ refers to the porosity function of the dynamic membrane and is defined as below [32]:

$$f(\varepsilon) = (1 - \varepsilon)^m \varepsilon^n \quad (4)$$

A lift force exerted on a particle due to mechanical agitation is defined as following equation [33]:

$$F_{L,Sa} = 6.46 \rho v_r d^2 \left(\frac{G\mu}{\rho} \right)^{0.5} \quad (5)$$

Mei [34] proposed the following approximate expression for the shear lift:

$$\frac{F_{L,Me}}{F_{L,Sa}} = 0.0524 \left(\frac{Gd}{v_r} \text{Re}_p \right)^{0.5} \quad (6)$$

The velocity and mean shear are determined by using the CFD simulation as before mentioned. As can be inferred from Eq. (6), the lift force exerted on a particle is a function of mixing intensity as well as the rotation speed of agitator. When the particles are dispersed in the continuous phase the adhesive forces declare its being as three main forces of Van der Waals, attractive or repulsive electrostatic, and liquid bridge [35]. Two solid particles molecularly establish attractive forces collectively known as van der Waals:

$$F_A = \frac{AR_1R_2}{6(R_1 + R_2)H^2} \quad (7)$$

where A is Hamakar constant and its value is approximately ranged to 20–25 ($\text{J} \times 10^{-20}$) for water and carbon and H is 0.4 nm [36]. The energy of the inter particle force can be written as below:

$$E = \frac{F_A}{d} \quad (8)$$

For activated carbon suspended in tap water, the order of magnitude for E becomes 1×10^{-3} N/m. The immobilization parameter, Im , as the ratio of the body forces and the adhesive force is defined as below:

$$Im = \frac{|F_D - F_L|}{F_A} = \frac{|kd\mu u \left(\frac{\delta}{d}\right) - F_{L,Me}|}{Ed} = \frac{k\mu u \left(\frac{\delta}{d}\right)}{E} - \frac{|F_{L,Me}|}{Ed} \quad (9)$$

with substituting Eqs. (3) and (4) into Eq. (9), the other state of the immobilization parameter becomes as follows:

$$Im = k \frac{\Delta P d^2}{EL} \frac{1}{(1 - \varepsilon)^{m+1} \varepsilon^n} \left(\frac{L}{d}\right) (1 - z) - \frac{F_{L,Me}}{Ed} \quad (10)$$

where the value of m and n indices is assumed to be equal to 1 and $-\varepsilon$, respectively. The dimensionless term $F_{D,A} = \frac{\Delta P d^2}{EL}$ demonstrates the force equilibrium due to fluid friction and intraparticle forces at the certain particle. The second term of Eq. (10) also demonstrates the effect of lift force due to flow field created by mechanical mixing. As inferred from Eq. (10), the porosity of dynamic membrane depends upon the parameters such as pressure drop across the layer of dynamic membrane, specific surface energy of particle, thickness of dynamic membrane, particle size, and the intensity of mechanical mixing. It can be resulted that Eq. (10) encompasses of two main terms: (1) the ratio between drag force and intraparticle force which is defined as drag dimensionless parameter, Im_D and (2) the ratio between lift force and intraparticle force, which is defined as lift dimensionless parameter, Im_L . The Eq. (10) can be ordered as below:

$$Im = Im_D - Im_L \quad (11)$$

4. Result and discussions

4.1. The velocity and shear rate calculated by CFD simulation

The predicted liquid velocity vector fields for two-phase (PAC–water) are shown in Fig. 5(a). Fig. 5(b) and (c) depicts the velocity and shear rate contours on a vertical surface with a 1 mm distance from dynamic membrane, respectively. The local vertical velocity profiles at distances 100–1,000 μm from the center of the membrane surface are represented in Table 2. As shown in Table 2, the local flow velocity increases slightly with distance from the dynamic membrane. It can be attributed to interaction between dynamic membrane surface and liquid phase in close proximity to membrane. The velocity profiles range from 0.116 to 0.122, 0.263 to 0.268, and 0.353 to 0.359 (m/s) for rotation speed of agitator 150, 300, and 450 rpm, respectively. The mean flow velocity and shear rate values obtained from the CFD simulation are applied to calculate the lift force exerted on particle.

4.2. Pre-coating dynamic membrane formation

Dynamic membrane is gradually formed by randomly deposition of suspended PAC particles on the mesh filter surface. The rotational speed of agitator varies at three values 150, 300, and 450 rpm upon which the just-complete suspension of PAC particles is performed. The SEM images are obtained to examine the dynamic membrane formation. As shown in Fig. 4(a), at the early stage of dynamic membrane formation, one layer of particles is almost formed on the surface of mesh filter and the spatial structure of first deposition layer is approximated to be in cubic form. The cross-section views obtained from SEM observation also display that the dynamic membranes are formed at different thicknesses including 100, 200, 300, 400, and 500 μm . The variations of pressure drop with prolonged pre-coating time are shown in Fig. 6. The results show that when developing the first layer of dynamic membrane at early stage of filtration, the TMP is moderately increased. Then, further development in the dynamic membrane formation results in higher TMP. The pre-coating time, which is defined as the interval between the time of start-up and the time when the TMP reaches stable and no significant change in TMP happens, is between 56 and 144 min in this study (dash line in Fig. 6). Before the pre-coating time, the thickness of dynamic membrane increases continuously, thus leading to increase in filtration pressure. The relationship between TMP and the thickness of dynamic membrane is also shown in

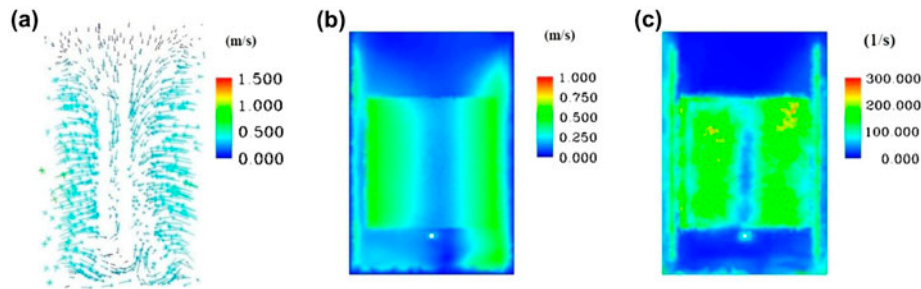


Fig. 5. (a) Liquid velocity vector fields for single-phase and (b), (c) the velocity and shear rate contours on a surface.

Table 2

Local velocity magnitudes at distances ranging from 100 to 1,000 μm from the center of the membrane surface

Distance from center of dynamic membrane (μm)		100	200	300	400	500	600	700	800	900	1,000
Velocity (m/s)	$N = 150 \text{ rpm}$	0.116	0.116	0.117	0.117	0.118	0.119	0.120	0.121	0.121	0.122
	$N = 300 \text{ rpm}$	0.263	0.264	0.264	0.265	0.266	0.266	0.267	0.267	0.268	0.268
	$N = 450 \text{ rpm}$	0.353	0.354	0.354	0.355	0.356	0.356	0.357	0.358	0.359	0.359

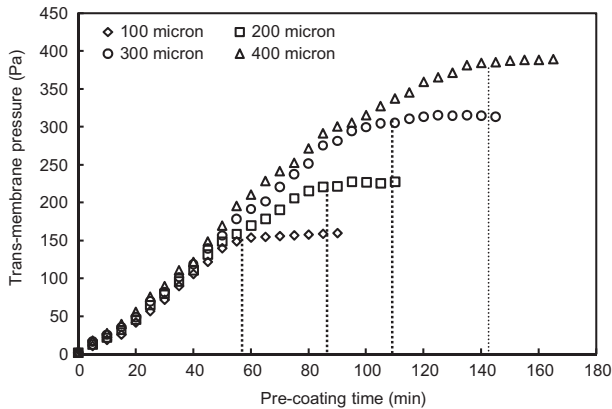


Fig. 6. Transmembrane pressure against pre-coating time.

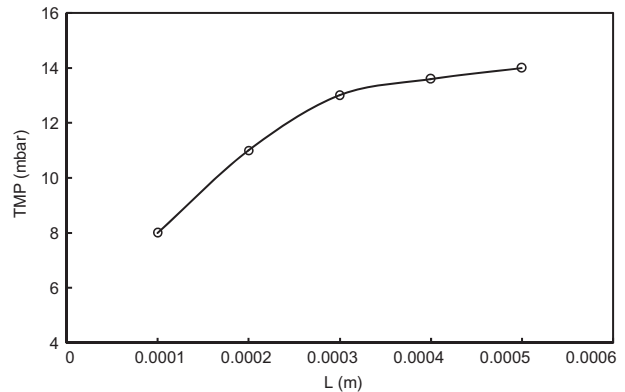


Fig. 7. Variations of TMP against different thicknesses of dynamic membrane.

Fig. 7. The TMP increases sharply in lower thickness ($\leq 300 \mu\text{m}$) and then increases slightly in higher thickness ($> 300 \mu\text{m}$) of dynamic membrane. The inflection point on curve is about $300 \mu\text{m}$. The difference in the trend of TMP variations can be due to the porosity and the morphology of dynamic membranes.

4.3. Effect of drag and lift forces on the porosity

The dimensionless term, $F_{D,A}$, as mentioned before is used as the representative of drag force to evaluate the effect of drag force owing to suction of permeate pump on the structure of dynamic membrane as well

as the porosity of dynamic membrane. Fig. 8 shows the variations of the porosity of dynamic membrane with the term, $F_{D,A}$ at various rotational speeds of agitator. As shown in Fig. 8, while this dimensionless term increases the porosity of dynamic membrane decreases. It can be said that the lower drag force results in the higher porosity of dynamic membrane, thereby occurring the looser dynamic membrane. It can also be concluded that the exerted drag force provides the stability of pre-coating dynamic membrane. In addition to Eq. (6), Sweeny's correlation [37] is used to calculate the lift force exerted on the particle. Fig. 9 compares the values of lift force obtained from Mei's

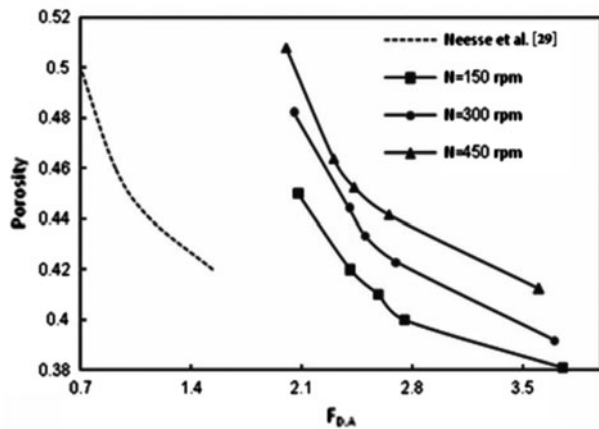


Fig. 8. Variation of porosity of dynamic membrane with drag force at different agitator revolution speeds.

and Sweeny’s correlations. Data obtained comes very close to each other with a linear regression slope of 0.91. The variations of the porosity of dynamic membrane with lift force are shown in Fig. 10 at different thicknesses of dynamic membrane. Lift force exerted on the particle strictly depends on the rotational speed of agitator. By increasing the speed of agitator, the mixing intensity increases so that the lift force on PAC particles increases. The denser dynamic membrane is formed when the lift force becomes lower. It can be resulted that the lift force on a particle affects the stability of pre-coating dynamic membrane.

4.4. Effect of the thickness of pre-coating dynamic membrane on the porosity

The porosity of dynamic membrane varies with thickness as illustrated in Fig. 11. The minimum

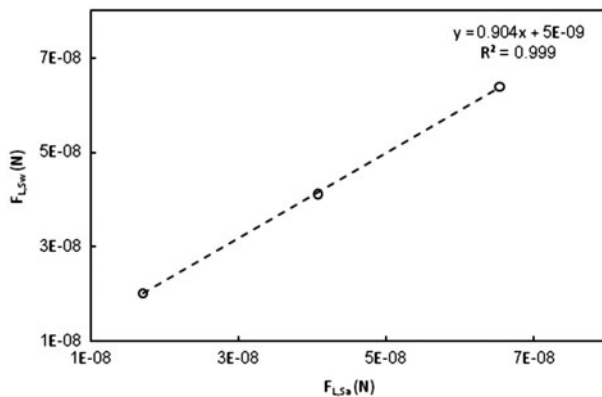


Fig. 9. Lift forces calculated by using Mei’s equation (F_L , M_e) and Sweeney’s correlation ($F_{L,Sw}$).

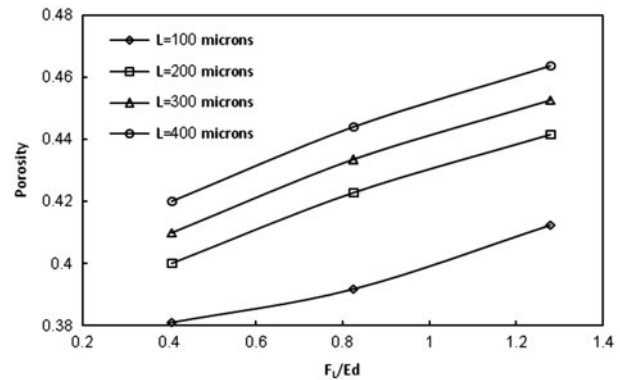


Fig. 10. Variation of porosity of dynamic membrane with lift force at various thicknesses.

porosity which is equal to 0.38 occurs at the thickness of 100 μm of dynamic membrane. As can be seen from Fig. 11, no significant change in the porosity is observed for the dynamic membrane with the thickness less than 400 μm . The porosity of dynamic membrane increases slightly with increasing the thickness till 400 μm and thereafter the porosity increases sharply with the thickness more than 400 μm . It can be resulted that the pre-coating dynamic membrane becomes denser at low thickness; therefore, it is looser at high thickness. The thickness of 400 μm can be considered as a threshold upon which the structure of dynamic membrane becomes unstable.

4.5. Immobilization parameter

As mentioned in Eq. (10), the dimensionless immobilization parameter encompasses of two major terms including the ratios of lift and drag forces over

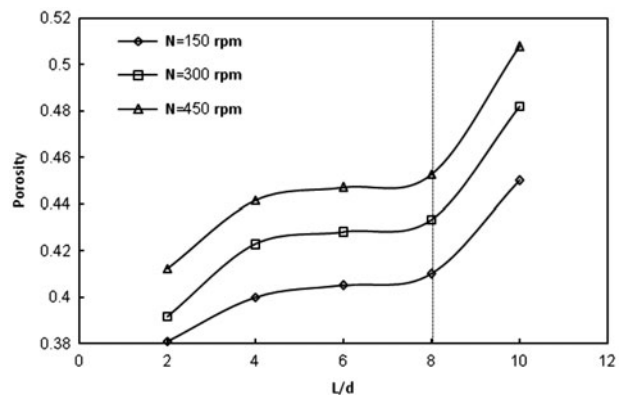


Fig. 11. Variation of porosity of dynamic membrane with the ration of thickness to particle diameter (L/d) at different agitator revolution speeds.

adhesive force. This parameter can be expected to be a theoretically appropriate criterion in order to predict the conditions of stable formation of the pre-coating dynamic membrane. Dynamic membrane which is formed at higher value of immobilization parameter ($Im > 1$) has a more cohesive structure; consequently it becomes more stable. As shown in Fig. 12, increasing the lift force due to mixing intensity decreases the value of immobilization parameter. On the other hand, the increase in the drag force due to shear stress of suction pump increases the value of the dimensionless parameter. It can be resulted that the dynamic membrane is steadily formed when the value of the immobilization parameter becomes more than unit. This parameter gets a value less than one for the dynamic membrane formed at the thickness of 500 μm at the revolution speed of 450 rpm, leading to weak structure of dynamic membrane. Experimental observations show that dynamic membrane formed at thickness of 500 μm is easily deformed under small shear.

4.6. Filtration capacity of PAC pre-coated dynamic membrane

A standard polymeric solution, Formazin solution, prepared according to ASTM standard method [38] is used to evaluate the filtration capability of the dynamic membrane forming on the mesh filter. Fig. 13 presents the turbidity effluent of the bare mesh filter and dynamic membranes when filtering the standard polymeric solution. As shown in Fig. 13, the mesh filter has low capacity to retain the suspended particles of Formazin solution and the filtrate quality of the bare mesh reaches 95 NTU. The results show that the presence of PAC layer as pre-coated dynamic

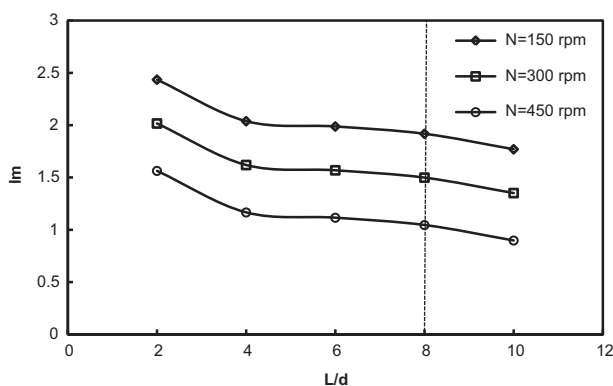


Fig. 12. Variation of immobilization index with the ration of thickness to particle diameter (L/d) at different agitator revolution speeds.

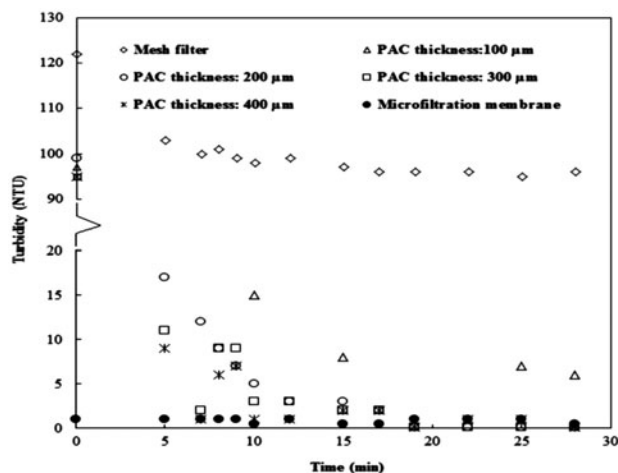


Fig. 13. The variations of filtrate turbidity at different thicknesses of dynamic membrane.

membrane improves the effluent quality. Notwithstanding the lower porosity obtained from the higher thickness of dynamic membrane, the filtrate quality improves when the thickness of dynamic membrane increases. It means that both porosity and thickness of dynamic membrane influence the filtration capacity in rejection of the particulate matter. As shown in Fig. 13, the filtrate turbidity of dynamic membranes decrease with filtration time at the beginning stage of filtration, then it reaches constant. At the end of filtration time, the effluent turbidity gets values less than 3 NTU and 1 NTU for dynamic membrane with thickness equal to 100 μm and more than 100 μm , respectively. The field observation also shows that the thin layer of milk-white on the external surface of the dynamic membrane is built-up at the early stage of filtration due to Formazin deposition. To compare the performance of pre-coating dynamic membrane with conventional membrane, a flat-sheet PVDF microfiltration membrane with average pore size 0.4 μm is used. The results reveal that rejection capacity of pre-coating dynamic membranes is comparable to that of PVDF microfiltration membrane (as shown in Fig. 13).

5. Conclusions

An *in situ* process is presented for formation of the pre-coating dynamic membrane. The dynamic membrane is formed at different thicknesses by deposition of mechanically suspended PAC particles on the mesh filter. The deposition of PAC particles on the mesh filter depends upon three main forces acting on a particle. The porosity of dynamic membrane as a function

of drag and lift forces is obtained. The results reveal that the porosity of dynamic membrane decreases with increasing drag force due to pump suction and with decreasing lift force due to mixing intensity. The dimensionless immobilization parameter is theoretically derived to predict the formation of pre-coating dynamic membrane. This parameter can appropriately determine the possibility of the formation of pre-coating dynamic membrane and its stability. The results demonstrate that higher value of immobilization parameter results in more stable structure of the pre-coating dynamic membrane. The results also reveal that the thickness of 400 μm is expected to be a threshold upon which the structure of dynamic membrane becomes unstable. In this case, the immobilization parameter value reaches unit. The results from the filtration of Formazin solution reveal that the dynamic membrane at higher thicknesses has better capacity in rejecting particular matters than lower thicknesses. The results also show that no significant change in rejection capacity is observed for the thicknesses of dynamic membrane more than 200 μm . The future study will be to characterize dynamic membrane formed by deposition of PAC on mesh filter in terms of required pre-coating time, the stages formation of dynamic membrane, intrinsically hydraulic resistance of dynamic membrane, pore size, and morphology of dynamic membrane.

List of symbols

F_D	— drag coefficient (N)
K	— constant coefficient (–)
U	— liquid velocity (m/s)
D	— particle diameter (m)
L	— final thickness of dynamic membrane (m)
Z	— dynamic membrane in z-direction (m)
z	— dimensionless parameter of thickness (Z/L)
ΔP	— pressure drop across dynamic membrane (Pa)
m, n	— exponents of porosity function (–)
$F_{L,Sa}$	— Saffman's lift force (N)
$F_{L,Me}$	— Mei's lift force (N)
$F_{L,Sw}$	— Sweeny's lift force (N)
v_r	— relative particle-liquid velocity (m/s)
G	— mean velocity shear of Saffman's equation (1/s)
Re_p	— Reynolds number of PAC particle (–)
F_A	— attractive force between two particles (N)
A	— Hamakar coefficient (J)
R_1, R_2	— radii of two particles (m)
H	— distance between two particles (m)
E	— energy of inter particle force (N/m)
Im	— immobilization parameter (–)
Im_D	— drag immobilization parameter (–)
Im_L	— lift immobilization parameter (–)
$F_{D,A}$	— ratio of fluid friction and inter particle forces (–)

Greek letters

δ	— specific layer of dynamic membrane (m)
μ	— liquid viscosity (Pa s)
ε	— porosity of dynamic membrane (–)
ρ	— liquid density (kg/m^3)

References

- [1] J.A. Howell, H.C. Chua, T.C. Amot, In situ manipulation of critical flux in a submerged membrane bioreactor using variable aeration rates and effects of membrane history, *J. Membr. Sci.* 242 (2004) 13–19.
- [2] E.J. McAdam, S.J. Judd, A review of membrane bioreactor potential for nitrate removal from drinking water, *Desalination* 196 (2006) 135–148.
- [3] T. Stephenson, S. Judd, B. Jefferson, K. Brindle, *Membrane Bioreactors for Wastewater Treatment*, IWA Publishing, London, 2000.
- [4] P. Le-Clech, V. Chen, T.A.G. Fane, Fouling in membrane bioreactors used in wastewater treatment, *J. Membr. Sci.* 284 (2006) 17–53.
- [5] Y. Zhang, Y. Zhao, H. Chu, B. Dong, X. Zhou, Characteristics of dynamic membrane filtration: structure, operation mechanisms, and cost analysis, *Chi. Sci. Bull.* 59 (2014) 247–260.
- [6] H. Chu, D. Cao, W. Jin, Characteristics of bio-diatomite dynamic membrane process for municipal wastewater treatment, *J. Membr. Sci.* 325 (2008) 271–276.
- [7] H. Chu, Y. Zhang, X. Zhou, Y. Zhao, B. Dong, H. Zhang, Dynamic membrane bioreactor for wastewater treatment: Operation, critical flux, and dynamic membrane structure, *J. Membr. Sci.* 450 (2014) 265–271.
- [8] M. Ye, H. Zhang, Q. Wei, H. Lei, F. Yang, X. Zhang, Study on the suitable thickness of a PAC-precoated dynamic membrane coupled with a bioreactor for municipal wastewater treatment, *Desalination* 194 (2006) 108–120.
- [9] B. Fan, X. Huang, Characteristics of a self-forming dynamic membrane coupled with a bioreactor for municipal wastewater treatment, *Environ. Sci. Technol.* 36 (2002) 5245–5251.
- [10] L. Chu, S. Li, Filtration capability and operational characteristics of dynamic membrane bioreactor for municipal wastewater treatment, *Sep. Purif. Technol.* 51 (2006) 173–179.
- [11] X. Zhang, Z.W. Wang, Z.C. Wu, F.H. Lu, J. Tong, L.L. Zang, Formation of dynamic membrane in an anaerobic membrane bioreactor for municipal wastewater treatment, *Chem. Eng. J.* 65 (2010) 175–183.
- [12] H. Liu, C. Yang, W. Puy, J. Zhang, Formation mechanism and structure of dynamic membrane in the dynamic membrane bioreactor, *Chem. Eng. J.* 148 (2009) 290–295.
- [13] A.A. Poostchi, M.R. Mehrnia, F. Rezvani, M.H. Sarrafzadeh, Low-cost monofilament mesh filter used in membrane bioreactor process: Filtration characteristics and resistance analysis, *Desalination* 286 (2012) 429–435.
- [14] F. Rezvani, M.R. Mehrnia, A.A. Poostchi, Optimal operating strategies of SFDM formation for MBR application, *Sep. Purif. Technol.* 124 (2014) 124–133.

- [15] H. Chu, B. Dong, Y. Zhang, X. Zhou, Gravity filtration performances of the bio-diatomite dynamic membrane reactor for slightly polluted surface water purification, *Water Sci. Technol.* 66 (2012) 1139–1146.
- [16] H. Chu, B. Dong, Y. Zhang, X. Zhou, Z. Yu, Pollutant removal mechanisms in a bio-diatomite dynamic membrane reactor for micro-polluted surface water purification, *Desalination* 293 (2012) 38–45.
- [17] M. Ye, H. Zhang, F. Yang, Experimental study on application of the boundary layer theory for estimating steady aeration intensity of pre-coated dynamic membrane bioreactors, *Desalination* 230 (2008) 100–112.
- [18] H. Chu, Y. Zhang, X. Zhou, B. Dong, Bio-enhanced powder-activated carbon dynamic membrane reactor for municipal wastewater treatment, *J. Membr. Sci.* 433 (2013) 126–134.
- [19] H. Park, K.-H. Choo, C.-H. Lee, Flux enhancement with powdered activated carbon addition in the membrane anaerobic bioreactor, *Sep. Sci. Technol.* 34 (1999) 2781–2792.
- [20] M. Pirbazari, V. Ravindran, B.N. Badriyha, S.H. Kim, Hybrid membrane filtration process for leachate treatment, *Water Res.* 30 (1996) 2691–2706.
- [21] H.H.P. Fang, X. Shi, T. Zhang, Effect of activated carbon on fouling of activated sludge filtration, *Desalination* 189 (2006) 193–199.
- [22] A.A. Poostchi, M.R. Mehrnia, M.H. Sarrafzadeh, Removal of dissolved organic carbon by multi-walled carbon nanotubes, powdered activated carbon and granular activated carbon, *Res. J. Chem. Environ.* 14 (2010) 59–66.
- [23] A. Akram, D.C. Stuckey, Flux and performance improvement in a submerged anaerobic membrane bioreactor (SABMR) using powdered activated carbon (PAC), *Process Biochem.* 43 (2008) 93–102.
- [24] H. Chu, Y. Zhang, B. Dong, X. Zhou, D. Cao, Z. Qiang, Z. Yu, H. Wang, Pretreatment of micro-polluted surface water with a biologically enhanced PAC–diatomite dynamic membrane reactor to produce drinking water, *Desalin. Water Treat.* 40 (2012) 84–91.
- [25] J. Ding, X. Wang, X.-F. Zhou, N.-Q. Ren, W.-Q. Guo, CFD optimization of continuous stirred-tank (CSTR) reactor for bio-hydrogen production, *Bioresour. Technol.* 101 (2010) 7016–7024.
- [26] M. Jahoda, L. Tomaskova, M. Mostek, CFD prediction of liquid homogenization in a gas–liquid stirred tank, *Chem. Eng. Res. Des.* 87 (2009) 460–467.
- [27] A.R. Khopkar, P.A. Tanguy, CFD simulation of gas–liquid flows in stirred vessel equipped with dual Rushton turbines: Influence of parallel, merging and diverging flow configurations, *Chem. Eng. Sci.* 63 (2008) 3810–3820.
- [28] E. Amini, M.R. Mehrnia, S.M. Mousavi, N. Mostoufi, Experimental study and computational fluid dynamics simulation of a full-scale membrane bioreactor for municipal wastewater treatment application, *Ind. Eng. Chem. Res.* 52 (2013) 9930–9939.
- [29] T.H. Neesse, J. Dueck, E. Djatchenko, Simulation of filter cake porosity in solid–liquid separation, *Powder Technol.* 193 (2009) 332–336.
- [30] G.G. Stokes, On the effect of the internal friction of fluids on the motion of the pendulums, *Trans. Cam. Phil. Soc.* 9 (1851) 8–27.
- [31] K. Gotoh, H. Masuda, K. Higashitani, *Powder Technology Handbook*, 2nd ed., Marcel Dekker, 1997.
- [32] J. Dueck, D. Purevjav, D.A. Kilimnik, Contribution to the theory of porosity of fine-grained sediments, *J. Eng. Phys. Thermophys.* 77 (2004) 93–102.
- [33] P.P. Saffman, The lift on a small sphere in a slow shear flow, *J. Fluid Mech.* 22 (1965) 385–400.
- [34] R. Mei, An approximative expression for the shear lift force on a spherical particle at finite Reynolds number, *Int. J. Multiphas. Flow* 18 (1992) 145–147.
- [35] A.D. Zimon, *Adhesion of Dust and Powder*, 2nd ed., Consultant Bureau, New York, NY, 1982.
- [36] W. Norde, *Colloids and Interfaces in Life Sciences*, Marcel Dekker, New York, NY, 2003.
- [37] L.G. Sweeney, W.H. Finaly, Lift and drag forces on a sphere attached to a wall in a Blasius boundary layer, *J. Aerosol Sci.* 38 (2007) 131–135.
- [38] Standard Test Method for Turbidity of Water, ASTM D 1889, 2000.